International Journal of Rotating Machinery 2005:3, 211–220

Systematic Investigation on Conjugate Heat Transfer Rates of Film Cooling Configurations

Dieter Bohn
Institute of Steam and Gas Turbines, Aachen University, Templergraben 55, 52056 Aachen, Germany
Email: post-bohn@idg.rwth-aachen.de

Jing Ren
Institute of Steam and Gas Turbines, Aachen University, Templergraben 55, 52056 Aachen, Germany
Email: jing@idg.rwth-aachen.de

Karsten Kusterer
B&B-AGEMA, Gesellschaft für Energietechnische Maschinen und Anlagen GmbH, Jülicher StraB 338, 52070 Aachen, Germany
Email: kusterer@bub-agema.de

Received 4 March 2005

For the determination of the film-cooling heat transfer, the design of a turbine blade relies on the conventional determination of the adiabatic film-cooling effectiveness and heat transfer conditions for test configurations. Thus, additional influences by the interaction of fluid flow and heat transfer and influences by additional convective heat transfer cannot be taken into account with sufficient accuracy. Within this paper, calculations of a film-cooled duct wall and a film-cooled real blade with application of the adiabatic and a conjugate heat transfer condition have been performed for different configurations. It can be shown that the application of the conjugate calculation method comprises the influence of heat transfer within the cooling film. The local heat transfer rate varies significantly depending on the local position.

Keywords and phrases: film cooling, shaped holes, conjugate heat transfer, secondary flows, specific heat rate.

1. INTRODUCTION

Due to high turbine inlet temperatures in gas turbine engines, film-cooling iswidely used for the vanes and blades of the front stages in order to reduce materialtemperatures to levels of required acceptable life span of each component. The cooling air is ejected through different rows of cooling holes with the objective of establishing a uniform continuous cooling film along the surface. In order to reduce the momentum of the ejected cooling air, holes with expanded exits are used for improved thermal protection of the blade. The performance of cooling can be expressed as the adiabatic cooling effectiveness, which is closely related to the velocity and temperature profiles as well as velocity and thermal boundary layer thickness.

Although the positive influence of shaped holes on film cooling is well known for a long time (e.g., Goldstein et al. [1]), a large number of papers has been published in recent years on this objective. The aim of the experimental and numerical studies is to receive a detailed understanding of the secondary flow development in the jets and to create a reliable database on the adiabatic film cooling effectiveness and heat transfer conditions. Detailed numerical analyses of the film cooling physics in the case of a flat plate with one row of cooling holes have been presented by Walters and Leylek [2] for cylindrical holes and by Hyams and Leylek [3] for shaped holes. Bohn and Moritz [4] have performed a numerical study on the influence of hole shaping of staggered multi-hole configurations on the cooling-film secondary flows.

Complex 3D numerical investigations for a real film-cooled blade have been presented by Garg and Rigby [5] with main interest in the hole exit regions and the heat transfer. Recent numerical studies on the leading edge film-cooling physics by York and Leylek [6, 7] focus on the determination of the adiabatic film cooling effectiveness and heat transfer coefficients. Bohn and Kusterer [8, 9] have investigated the 3D cooling jet phenomena for blade leading edge ejection from nonlateral and radially inclined cooling holes.

Numerical investigations within this paper deal with a hot gas duct flow with one row of cooling holes. The hole geometry comprises different configurations with cylindrical holes and shaped exits (diffuser and fan-shaped). The calculations include the supply channel of the holes and have been performed by application of the CHTflow solver developed by the Institute of Steam and Gas Turbines at Aachen University.

Within the calculations, the adiabatic wall boundary condition as well as the conjugate heat transfer boundary condition have been used. The main focus of this paper is to show the influence of the more realistic conjugate heat transfer on the local specific heat flux distribution. It will be shown that the application of the conjugate method includes the influence of heat transfer on the cooling film. Thus, it becomes obvious that when applying heat transfer boundary conditions for numerical simulations based on conventional adiabatic analysis or fixed thermal boundary conditions, these effects cannot be taken into account.

2. CONVENTIONAL HEAT TRANSFER DETERMINATION

With respect to most of the experimental studies (e.g., Gritsch et al. [10], Lutum et al. [11], Reiss and Bölcs [12], Yuen et al. [13]), the determination of the adiabatic film cooling effectiveness is of main importance. The adiabatic film cooling effectiveness is one of the two important parameters of the conventional approach for the determination of the heat transfer rate:

$$q = h_f(T_w - T_{aw}). \tag{1}$$

Here h_f is the film heat transfer coefficient, T_w is the wall temperature, and T_{aw}, the adiabatic wall temperature in the case of film cooling, serves as a reference temperature (Table 1). The heat transfer coefficient h_f considers the influence of the film cooling on the local heat transfer due to the modified flow field. Without film cooling, T_{aw} will be the recovery temperature T_r of the hot gas flow. The performance of cooling can be expressed as the adiabatic film cooling effectiveness:

$$\eta_f = \frac{T_{aw} - T_r}{T_{oc} - T_r}. \tag{2}$$

HereT_{oc} is the stagnation temperature of the cooling fluid near entry (Table 1). If the adiabatic cooling effectiveness is known, the adiabatic wall temperature can be determined, but, for the solution of (1), the knowledge of the film heat transfer coefficient is also necessary. Experiments with constant and defined heat transfer rates (e.g., Lutum et al. [11]) give the possibility of determining these coefficients.

Within numerical simulations, similar conventional approaches are used for analyzing the heat transfer of a turbine blade. Thus, isothermal or constant heat flux conditions are prescribed at the blade surface. With respect to the film-cooling case (a two-temperature problem), two different external flow conditions are used for the calculation of the heat transfer coefficient and film-cooling effectiveness distributions, which then can be used for FEM calculations in order to obtain the solid temperature distributions. Unfortunately, these methods decouple the fluid solution from the thermal conduction in the solid and assume that thermal boundary conditions at the walls do not influence the heat transfer coefficient and film cooling effectiveness distributions. It can be found in literature (e.g., Kays and Crawford [14]) that this assumption might be fair for turbulent flat plate flows. But, for the cases of modern film-cooled turbine blades, we will find very inhomogeneous local heat flux distributions with high peak values and, thus, the assumptions and simplifications of the conventional approaches are likely only to be valid for a first approach. Local influences of heat transfer on the flow and vice verse might be greater than expected.

3. CONJUGATE CALCULATION TECHNIQUE

As discussed above, the conventional approaches on the heat transfer determination suffer from some uncertainties and inaccuracies, in particular, if the data is transferred to the real blade flow. The interaction of the heat transfer and the fluid flow is of importance for the precise determination of the heat transfer. Furthermore, for a real blade the additional convective cooling effects are also of importance. One main effect is that the cooling fluid is heated convectively on the way through the supply channels and the cooling holes. Thus, the cooling fluid condition at the hole exit varies with the internal heat transfer and, furthermore, has an influence on the external cooling performance.

For the numerical simulation, the conjugate calculation technique used in the CHTflow code (e.g., Bohn et al. [15, 16, 17]) offers the opportunity to avoid the use of the film-cooling heat transfer boundary conditions and allows a direct coupled calculation of the heat transfer and the wall temperatures. The numerical scheme for the simulation of the fluid flow and heat transfer works on the basis of an implicit finite-volume method combined with a multiblock technique. The physical domain is divided into separate blocks for the fluid and solid body regions. Full, compressible, three-dimensional Navier-Stokes equations are solved in the fluid blocks. The closure of the Reynolds averaged equations is provided by the Baldwin-Lomax algebraic eddy-viscosity turbulence model (Baldwin and Lamax [18]).

The Fourier equation is solved in the solid body blocks. Coupling of fluid blocks and solid body blocks is achieved via a common wall temperature resulting from the equality of the local heat fluxes passing through the contacting cell faces. This means that no heat transfer boundary conditions have to be stipulated on the solid surfaces as in conventional numerical simulation without the conjugate technique. This method of calculating the heat fluxes requires a very high grid resolution at the contacting block faces. In particular, the numerical grid for the fluid flow calculation should allow an

Table 1: Nomenclature.

Symbol	Unit of measurement	Notation
c	ms^{-1}	Velocity
D	mm	Diameter
h	$Wm^{-2}K^{-1}$	Heat transfer coefficient
M	—	Blowing ratio
q	Wm^{-2}	Specific heat flux rate
T	K	Temperature
x	mm	Streamwise coordinate
y	mm	Coordinate perpendicular to wall
ρ	kgm^{-3}	Density
θ	—	Nondimensional temperature
λ	$Wm^{-1}K^{-1}$	Conductivity
η_f	—	Adiabatic film effectiveness
Subscripts		
a		Adiabatic
c		Cooling
f		Film cooling
g		Hot gas
iso		Difference value between two isolines
o		Stagnation
r		Recovery
w		Wall

adequate resolution of the laminar sublayer. The use of a principally identical formulation and solution of the energy equation in the solid body blocks as in the fluid blocks is advantageous for the implementation and stability of the couplingprocedure (homogeneous method). Other conjugate calculation approaches have been presented also by several authors (e.g., Kao and Liou [19], Han et al. [20], Montenay et al. [21], Li and Kassab [22], Okita and Yamawaki [23], Heidmann et al. [24], York and Leylek [25]).

4. HOT GAS DUCT

4.1. Geometric configuration

In this study, a hot gas duct flow with cooling fluid injection through onerow of 8 cooling holes shown in Figure 1 is numerically investigated. The hole geometry comprises of three different configurations of cylindrical holes and shaped exits (diffuser and fanshaped).

An analysis with two different heat transfer boundary conditions is performed for the duct wall with cooling fluid ejection. The first part (holes no. 1 to no. 4) is calculated with the conjugate heat transfer condition. Thus, heat fluxes between the fluid flow and the solid body and vice versa are calculated directly. The second half of the wall (holes no. 5 to no. 8) is calculated with the adiabatic wall condition. A supply of cooling fluid for the holes is reached by a rectangular duct from one side with a 90° angle to the streamwise direction. Therefore, the situation of the hole inflow is similar to the supply of cooling holes in real blade configurations. At the end of the rectangular cooling duct a small exit hole similar to a blade tip hole is part of the calculation. The geometry of the duct and the solution domain are illustrated in Figure 1. Figure 2 shows the hole configuration and their basic parameters. The hole diameter is $D = 1$ mm and the hole spacing is $P/D = 3$.

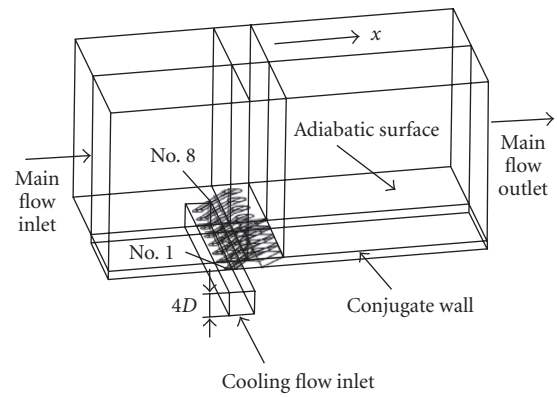

Figure 1: Duct geometry and solution domain.

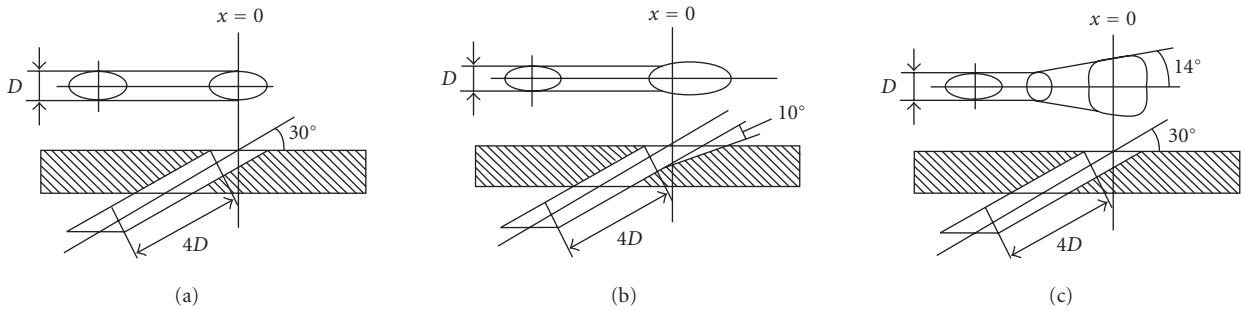

Figure 2: Illustration of the hole configurations: (a) cylindrical hole, (b) diffuser hole, and (c) fanshaped hole.

Table 2: Boundary conditions ($M = 2.0$).

Parameter	Main flow	Cooling flow
Inlet density (kg/m^3)	2.78	6.96
Inlet velocity (m/s)	256.0	65.0
Outlet pressure (Pa)	11.2×10^5	13.2×10^5

4.2. Boundary condition

The inlet mass flows for the hot gas channel and the cooling supply are fixed preciselyby the boundary conditions. Therefore, the blowing ratio

$$M = \frac{\rho_c c_c}{\rho_g c_g}, \tag{3}$$

which is the ratio of density and velocity values for the cooling flow and the hot gas flow, has been set to certain values ($M = 1.0$, $M = 1.5$, $M = 2.0$) for the holes of all configurations. Table 2 gives the boundary conditions for the $M = 2.0$ case as an example.

4.3. Numerical results and discussion

This part of theresults deals with the temperature distribution in thecooling jets and the determination of the specific heat flux rate. Figure 3 gives an illustration of the dimensionless flow temperature in different axial cutting planes for the two cooling jets in the middle of the duct (no. 4 and no. 5) in the case for $M = 2.0$. The cylindrical hole ejection shows a lift-off of the cooling jet and, thus, the core of the jet is not close to the wall and hot gas contact occurs between the jets. For the conjugate part, heat fluxes from the hot main flowinto the wall between the jets lead to heating up of the solid body. At the position of the cooling jets, heat transfer from the hot wall into the cooling jets occurs, which leads to an additional temperature increase of the cooling jet in comparison to the adiabatic part.

The ejection with diffuser-shaped holes shows that the cores of the cooling jets are now close to the wall and the lift-off of the jets is avoided. Furthermore, the cooling jets spread out slightly into the lateral direction leading to reduced hot gas contact between the jets.

Due to the conjugate wall condition, the cooling jet no. 4 heats up more quickly than jet no. 5 of the adiabatic side. The fanshaped configuration leads to a significantly improved cooling film as the lateral extension of the jets is further increased.

Figure 4 shows for the adiabatic surface of the duct wall the adiabatic cooling effectiveness. In the case of the conjugate part of wall, the values of the effectiveness give a nondimensional surface wall temperature. The adiabatic effectiveness shows the significant improvement of the cooling performance for the shaped configurations whereas the lift-off in the cylindrical case leads to a very poor performance. Furthermore, the improved lateral extension of the single jets for the fanshaped configuration keeps only a very narrow region of reduced performance between the jets.

For the conjugate part, the effectiveness value of 0.2 for the cylindrical hole ejection means that only 20% of the cooling potential (temperature difference between the main flow adiabatic wall temperature and the stagnation temperature of cooling fluid) is used whereas for the diffuser-shaped holes it is over 40%. The fanshaped configuration leads to effectiveness values, which are over 60% close to the hole outlets.

For the conjugate part of the calculations, it is possible to determine the specific heat flux rate q from the local gradient in the thermal boundary layer:

$$q = -\lambda \frac{\partial T}{\partial y}\bigg|_w. \tag{4}$$

Figure 5 illustrates the local distribution of the specific heat flux rate for the conjugate wall of the three configurations when the blowing ratio equals 2.0. The region of special interest is in the hole exit area. At first, it has to be stated that there exist regions with heat transfer from the flow into the duct wall (negative "blue" values) and regions with heat transfer from the wall to the duct flow (positive values). The latter regions correspond to regions with a high adiabatic cooling effectiveness as in these regions the local fluid temperatures are lower than the wall temperatures. There is a significant variation in the levels of the heat flux rate with highest positive values to be found directly downstream of the hole exits. The high density of isolines between the cooling jets indicates the regions of hot gas contact.

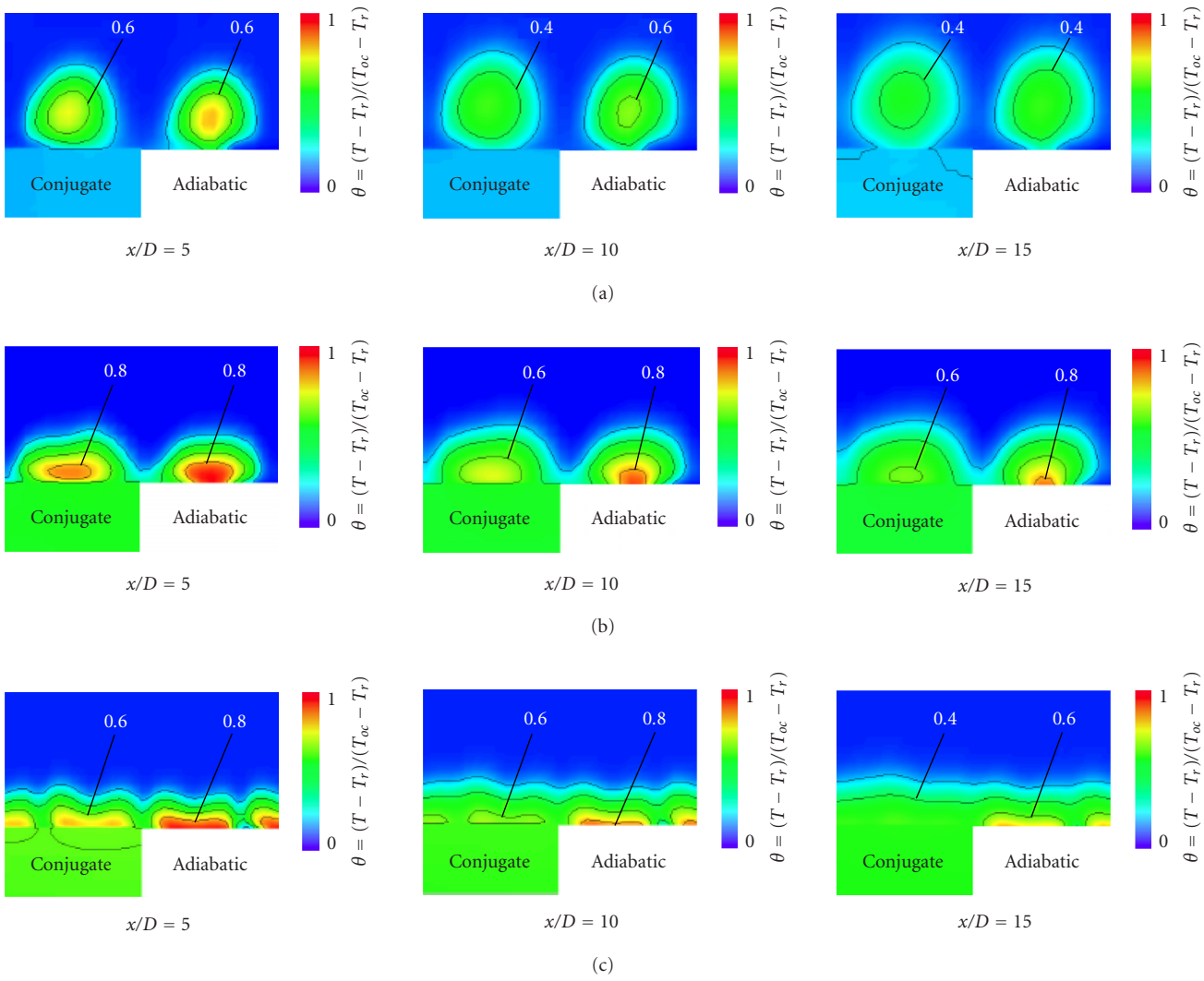

FIGURE 3: Nondimensional temperature distribution in x = const. Planes (M = 2.0): (a) cylindrical hole (ΔT_{iso} = 0.2), (b) diffuser hole (ΔT_{iso} = 0.2), and (c) fanshaped hole (ΔT_{iso} = 0.2).

Although the local variation of the specific heat flux rate is very large, the nondimensionaltemperature distribution on the conjugate surface in Figure 3 has been found to be very homogeneous. The reason is the high heat conduction into the lateral direction within the duct wall. The temperature distribution in the wall and, in particular, the level of the wall temperature results from the conjugate solution for the equilibrium state of heat flux into the wall and out of the wall.

Due to the fact that in the numerical model no additional internal cooling or nonadiabatic boundary conditions have been established, which can transport the heat out of the system, the amount of heat taken up by the conjugate duct wall has to be transferred back to the duct flow in the regions of locally low flow temperatures at the surface. For the cylindrical hole configuration this leads to moderate heat transfer rates upstream the holes and in the downstream region of low cooling efficiencies. High positive values exist only in the small region of direct cooling fluid contact in the downstream vicinity of the hole exits.

As the cooling of the duct wall becomes more efficient for the shaped hole configurations, the negative value of the specific heat rate in front of the hole exits increases. In particular for the fanshaped configuration, the contact area for the duct wall with "cold" main flow has been increased significantly. As a result, the amount of heat to be transferred back to the main flow distributes on a larger area and, thus, the positive local values of the specific heat flux rate are distinctly lower in comparison to the cylindrical hole configuration. Furthermore, the homogeneous distribution of the specific heat rate at a low level also proves the good cooling performance of the fanshaped configuration.

Figure 6 illustrates the local distribution of the specific heat flux rate for the conjugate wall of the three configurations when the blowing ratio is at a lower value (M = 1.0). As it is expected, the quantitative values for the specific heat

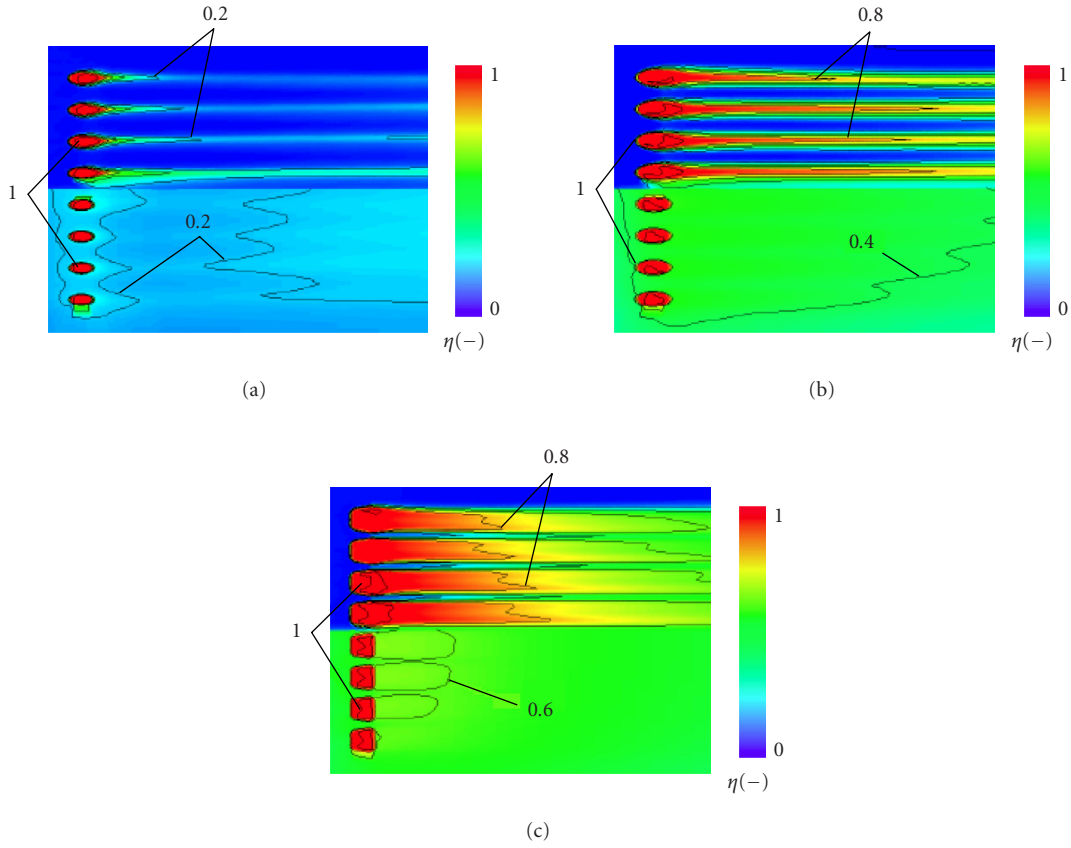

FIGURE 4: Cooling effectiveness distribution on the wall surface ($M = 2.0$, $\Delta\eta_{iso} = 0.2$): (a) cylindrical hole, (b) diffuser hole, and (c) fanshaped hole.

transfer rates are lower than in the $M = 2.0$ case. But, with respect to the qualitative appearance of the distributions, no significant differences can be detected. In the case of the fanshaped configuration, the heat flux distribution turns out to be much more homogeneous than the distributions for the other two configurations. The reasons are the same as discussed for the $M = 2.0$ case of Figure 5. All peak values are lower than for the high blowing ratio case.

5. FILM-COOLED BLADE

5.1. Test configuration

Based on an experimental test configuration, developed by Kawasaki Heavy Industries (KHI), Ltd. for the film cooling of a first-stage blade of a modern gas turbine (Sugimoto et al. [26]), further numerical investigations on the specific heat flux rates for a real blade cooling configuration have been performed.

At the blade leading edge, the configuration consists of three rows of radically inclined cooling holes (indicated as "P1," "LE," and "S1" in Figure 7a), which are supplied by a single cooling channel. Furthermore, the experimental test configuration also includes two rows of shaped holes, one on the suction side (indicated as "S2") and one on the pressure side (indicated as "P2"), respectively, supplied by further internal cooling passages as shown in Figure 7b. The trailing edge chamber is supplied by channel no. III through several crossover holes before the cooling air is ejected through a row of small slots at the trailing edge.

5.2. Conjugate models for the film-cooled blade

Due to the complexity of the complete configuration, it has been decided to divide the conjugate calculation into two different tasks in order to reduce the calculation effort. Task 1 deals with the modeling and simulation of the leading edge cooling, whereas Task 2 neglects the leading edge ejection and the leading edge supply channel.

Model for leading edge simulation (Task 1)—Figure 8a

For the conjugate calculation of the leading edge region, a 3D numerical grid consisting of nearly 3.1 million grid points in 181 blocks has been generated. The numerical grid consists of the complete blade passage, the radial gap in a simplified model, all cooling holes of the three rows at the leading edge (altogether 42 holes), and the leading edge supply channel. The internal walls have been modeled as smooth walls. Additional solid body blocks in the leading edge region have been included in the model. Therefore, direct coupling of the solid body and the fluid flow regions is established in the leading edge region and the internal and external heat

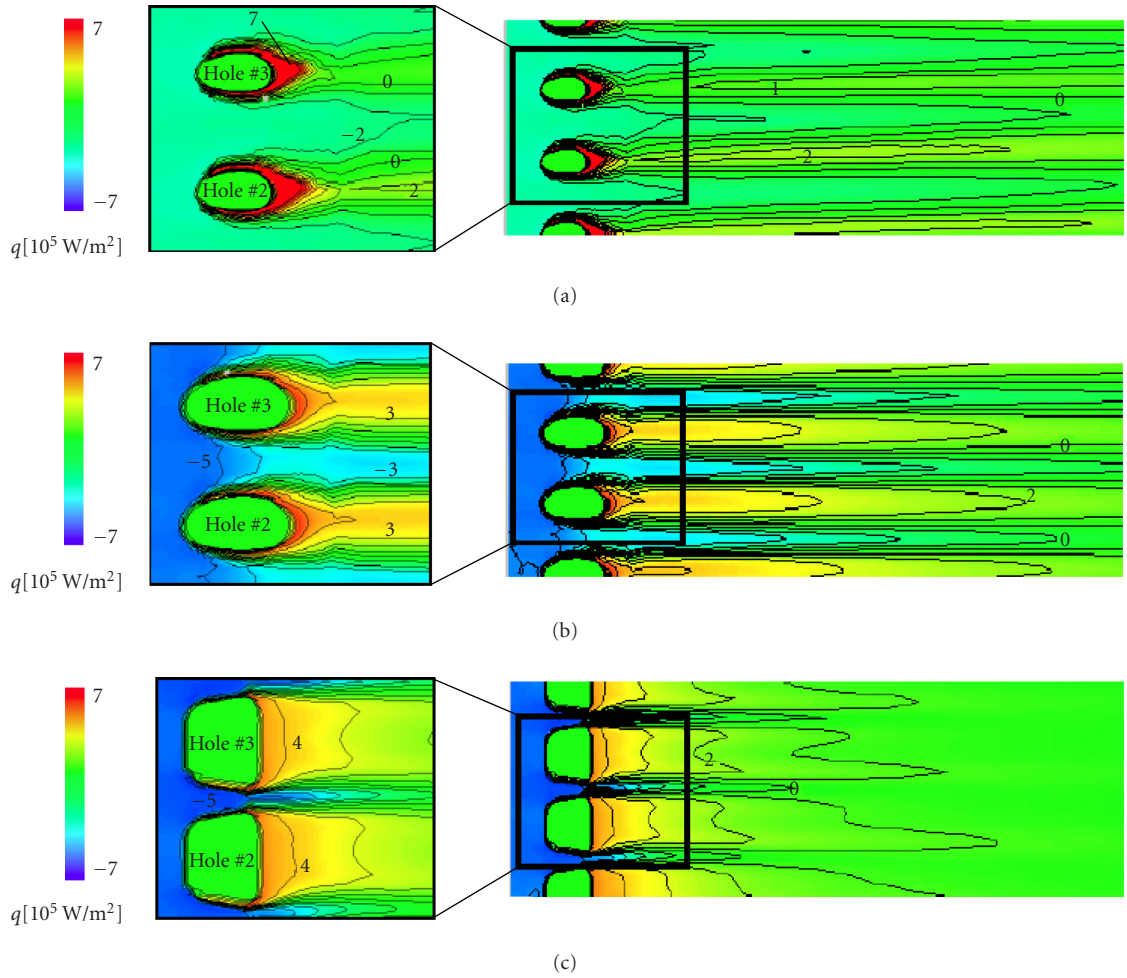

Figure 5: Distribution of the specific heat flux rate for the conjugate surface ($M = 2.0$): (a) cylindrical hole, (b) diffuser hole, and (c) fanshaped hole.

transfer is taken into account during the calculation. At the internal solid body boundary a fixed temperature has been prescribed. Thus, it will be possible to consider the effects of this fixed boundary condition, when the thermal load at the leading edge is investigated.

Model without leading edge cooling (Task 2)—Figure 8b

For the conjugate calculations, a 3D numerical grid consisting of nearly 4.4 million grid points in 253 blocks has been generated. The numerical grid consists of the blade internal passages (except leading edge passage), the radial gap (complex model including the tip outlets), all cooling holes of the suction side row with shaped holes, pressure side row with shaped holes, and the trailing edge row of ejection slots. The trailing edge chamber has been modeled without the pin fins and all passage walls have been calculated as smooth walls.

With respect to the conjugate calculation, the solid blocks for the blade itself have been limited to the upper part of the blade. Thus, the blade is divided into an adiabatic lower part and a full-conjugate upper part, similar to the model for the duct wall investigations presented in the first part of the paper.

5.3. Results on specific heat flux distributions

Task 1 (leading edge cooling). Figure 9 illustrates the local distribution of the specific heat flux rate for the conjugate wall of the leading edge region of the blade. It can be shown that the distribution of the specific heat flux rate is very inhomogeneous in this region. Regions with heat transfer from the flow into the blade wall (negative "blue" values) exist directly in the stagnation area. Regions with heat transfer from the wall to the external flow (positive "red" values) are to be found downstream the cooling holes where wall contact of the cooling film is established. In particular, in the vicinity of the holes very high positive heat flux rates up to 1.6E6 W/m^2 can occur. The maximum negative values in the stagnation region are up to 1.2E6 W/m^2. As the local conjugate wall temperatures are the result of the coupled calculation of convective internal cooling, the heat conduction in the blade material and the external heat transfer, the distribution of the

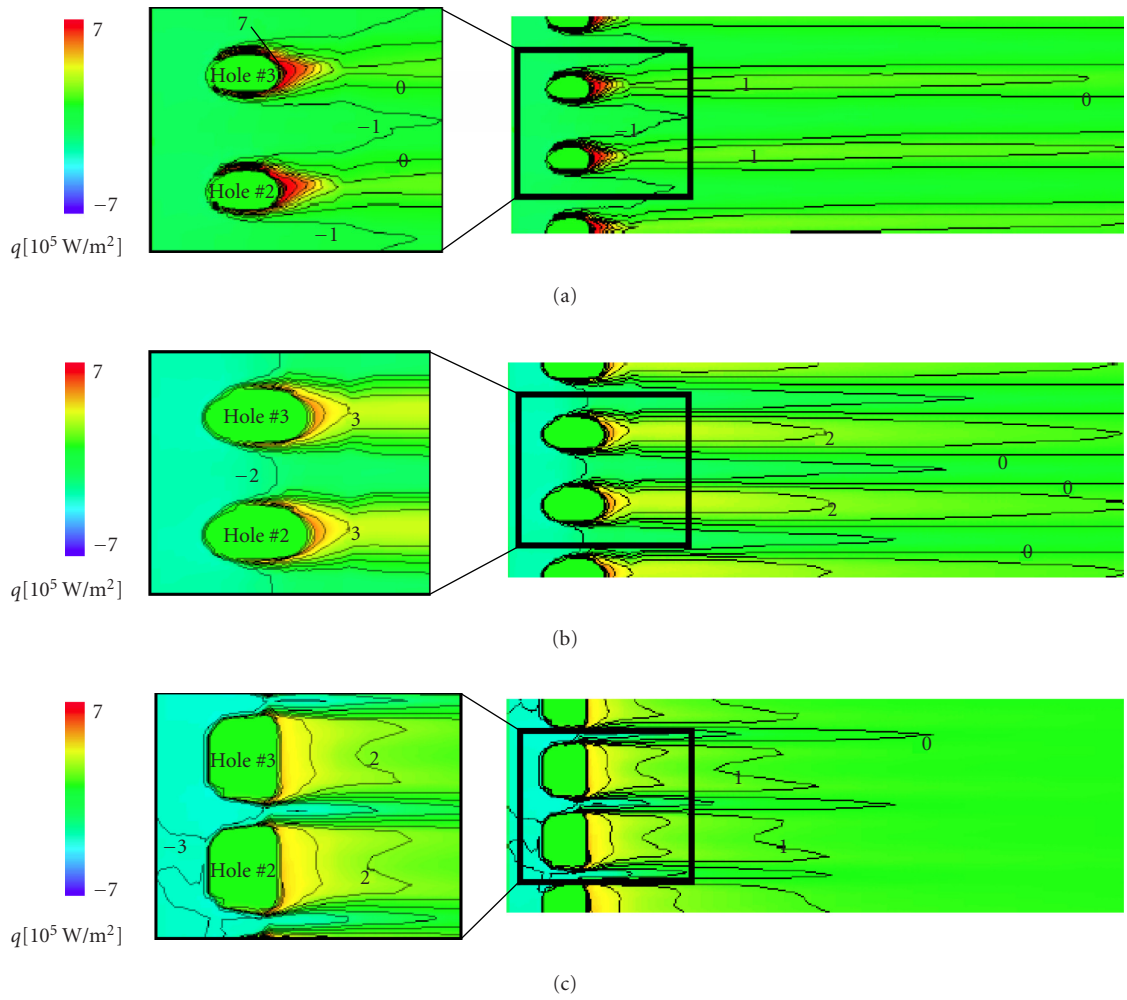

Figure 6: Distribution of the specific heat flux rate for the conjugate surface ($M = 1.0$): (a) cylindrical hole, (b) diffuser hole, and (c) fanshaped hole.

heat transfer rate is more realistic than calculations by conventional numerical tools based on heat transfer boundary conditions.

Task 2 (blade tip cooling). The visualization of the specific heat transfer rate in Figure 10 shows that for the shaped-holes on the suction side the distribution of the heat transfer becomes more homogeneous because a direct contact with the cooling fluid is established downstream the holes. Therefore, the level of the positive and negative values of the heat transfer rate is also reduced. The region with a positive heat transfer rate near the tip of the blade is established by cooling fluid ejected to the radial gap of the blade.

The results for the specific heat flux rates of both tasks show that for real blade configurations similar distributions can be obtained than for the simpler duct flow case. It becomes obvious that in the vicinity of the cooling holes and downstream of the cooling air ejection the highest inhomogeneity in the heat flux rates with peak levels can be expected. Thus, it is very likely that the ejection conditions are affected by the local heat transfer.

6. CONCLUSIONS

Numerical simulations of a duct flow with cooling fluid injection through different hole configurations as well as simulations of a film-cooled blade have been performed. Within the same calculation, the conjugate heat transfer condition and the adiabatic wall condition have been applied to one half of the objects and to the other half, respectively. The results confirm that the conjugate calculation can take into account the mutual influences of heat transfer on the fluid flow and vice versa due to the more realistic distribution of the local heat fluxes. The thermal analysis shows the effect of the conjugate heat transfer on the temperature field in the cooling film and, thus, the additional heating up of the cooling jet can be shown. With respect to the adiabatic cooling effectiveness, which can be calculated for the adiabatic part of the

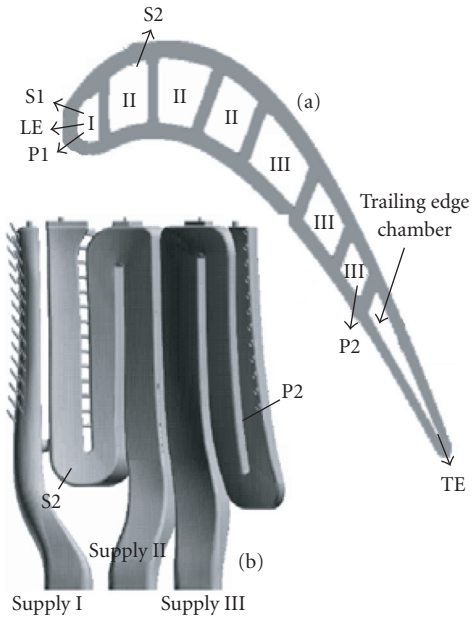

Figure 7: Film-cooled test blade: (a) mid-section of test configuration, (b) internal cooling system (without trailing edge chamber).

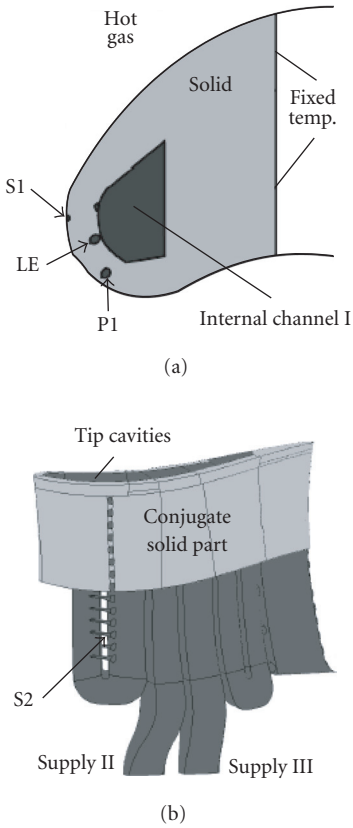

Figure 8: Numerical models of blade geometry. (a) Task 1: leading edge cooling model. (b) Task 2: model without leading edge cooling.

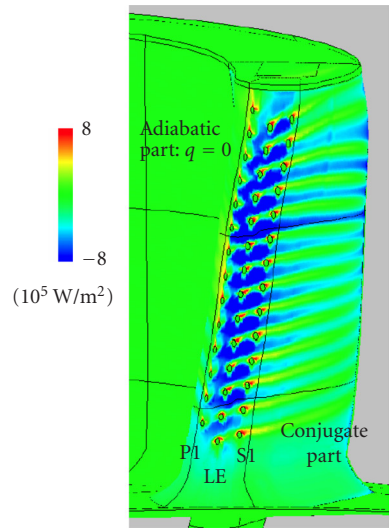

Figure 9: Specific heat transfer distribution at the leading edge.

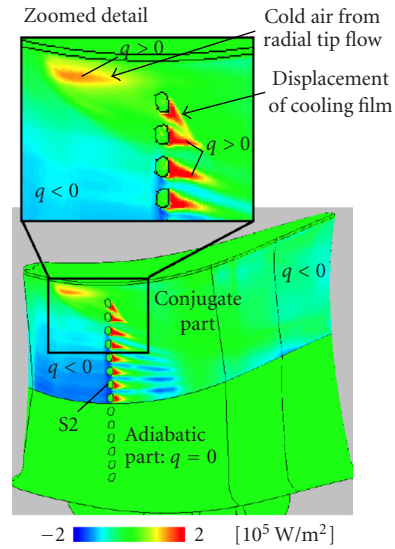

Figure 10: Specific heat transfer rate distribution on the suction side.

wall, the superiority of the fanshaped configuration becomes evident. For the conjugate part, the calculated effectiveness represents the direct cooling performance with respect to the established wall temperatures. Thus, it can be shown that the fanshaped configuration is up to three-time effective than the cylindrical hole configuration. A large variation in the level of the local specific heat flux rate exists for the conjugate wall. An increase in the film-cooling performance is connected to a more homogeneous distribution of the heat flux rate. The specific heat flux distributions for a real bladeconfiguration show more similar characteristics than the distributions for a simpler test case with one film-cooled duct wall.

REFERENCES

[1] R. J. Goldstein, E. R. G. Eckert, and F. Burggraff, "Effects of hole geometry and density on three-dimensional film cooling," *International Journal of Heat and Mass Transfer*, vol. 17, pp. 595–607, 1974.

[2] D. K. Walters and J. H. Leylek, "A detailed analysis of film-cooling physics part I: streamwise injection with cylindrical holes," ASME-paper 97-GT-269, American Society of Mechanical Engineers, Orlando, Fla, USA, 1997.

[3] D. G. Hyams and J. H. Leylek, "A detailed analysis of film-cooling physics part II: streamwise injection with shaped holes," ASME-paper 97-GT-271, American Society of Mechanical Engineers, Orlando, Fla, USA, 1997.

[4] D. Bohn and N. Moritz, "Influence of hole shaping of staggered multi-hole configurations on cooling film development," in *Proc. AIAA 34th Thermophysics Conference*, pp. 1–10, Denver, Colo, USA, June 2000, paper 2000-2579.

[5] V. K. Garg and D. L. Rigby, "Heat transfer on a film-cooled blade—effect of hole physics," *International Journal of Heat and Fluid Flow*, vol. 20, no. 1, pp. 10–25, 1999.

[6] W. D. York and J. H. Leylek, "Leading-edge film-cooling physics: part I—adiabatic effectiveness," ASME-paper GT-2002-30166, American Society of Mechanical Engineers, Orlando, Fla, USA, 2002.

[7] W. D. York and J. H. Leylek, "Leading-edge film-cooling physics: part II—heat transfer coefficient," ASME-paper GT-2002-30167, American Society of Mechanical Engineers, Orlando, Fla, USA, 2002.

[8] D. Bohn and K. Kusterer, "Blowing ratio influence on jet mixing flow phenomena at the Leading Fdge," AIAA-paper 99-0670, American Institute of Aeronautics and Astronautics, Reno, Nev, USA, 1999.

[9] D. Bohn and K. Kusterer, "Aerothermal investigations of mixing flow phenomena in case of radially inclined ejection holes at the leading edge," *Journal of Turbomachinery*, vol. 122, no. 2, pp. 334–339, 2000.

[10] M. Gritsch, A. Schulz, and S. Wittig, "Adiabatic wall measurements of film-cooling holes with expanded exits," *Journal of Turbomachinery*, vol. 120, pp. 568–574, 1998.

[11] E. Lutum, J. von Wolfersdorf, K. Semmler, J. Dittmar, and B. Weigand, "An experimental investigation of film cooling on a convex surface subjected to favourable pressure gradient flow," *International Journal of Heat and Mass Transfer*, vol. 44, no. 5, pp. 939–951, 2001.

[12] H. Reiss and A. Bölcs, "The influence of the boundary layer state and Reynolds number on film cooling and heat transfer on a cooled nozzle guide vane," ASME-paper 2000-GT-205, American Society of Mechanical Engineers, Orlando, Fla, USA, 2000.

[13] C. H. N. Yuen, R. F. Martinez-Botas, and J. H. Whitelaw, "Film-cooling effectiveness downstream of compound and fan-shaped holes," ASME-paper 2001-GT-0131, American Society of Mechanical Engineers, Orlando, Fla, USA, 2001.

[14] W. M. Kays and M. E. Crawford, *Convective Heat and Mass Transfer*, McGraw-Hill, New York, NY, USA, 2nd edition, 1980.

[15] D. Bohn and B. Bonhoff, "Berechnung der Kühl- und Störwirkung eines filmgekühlten transonisch durchströmten Turbinengitters mit diabaten Wänden," *VDI-Bericht*, vol. 1109, pp. 261–275, 1994 (Germany).

[16] D. Bohn, B. Bonhoff, H. Schönenborn, and H. Wilhelmi, "Validation of a numerical model for the coupled simulation of fluid flow and diabatic walls with application to film-cooled turbine blades," *VDI-Bericht*, vol. 1186, pp. 295–272, 1995 (Germany).

[17] D. Bohn, U. Krüger, and K. Kusterer, "Conjugate heat transfer: an advanced computational method for the cooling design of modern gas turbine blades and vanes, in: heat transfer in gas turbines," in *Heat Transfer in Gas Turbines*, B. Sunden and M. Faghri, Eds., pp. 55–108, WIT Press, Southampton, UK, 2001.

[18] B. S. Baldwin and H. J. Lomax, "Thin layer approximation and algebraic model for separated turbulent flows," in *Proc. 16th Aerospace Sciences Meeting*, huntsville, Ala, USA, January 1978, paper 78-257.

[19] K.-H. Kao and M.-S. Liou, "On the application of chimera/unstructured hybrid grids for the conjugate heat transfer," ASME-paper 96-GT-156, American Society of Mechanical Engineers, Orlando, Fla, USA, 1996.

[20] Z.-X. Han, B. H. Dennis, and G. S. Dulikravich, "Simultaneous prediction of external flow-field and temperature in internally cooled 3-D turbine blade material," ASME-paper 2000-GT-253, American Society of Mechanical Engineers, Orlando, Fla, USA, 2000.

[21] A. Montenay, L. Paté, and J. M. Duboué, "Conjugate heat transfer analysis of an engine internal cavity," ASME-paper 2000-GT-282, American Society of Mechanical Engineers, Orlando, Fla, USA, 2000.

[22] H. Li and A. J. Kassab, "Numerical prediction of fluid flow and heat transfer in turbine blades with internal cooling," AIAA-paper 94-2933, American Institute of Aeronautics and Astronautics, Reno, Nev, USA, 1994.

[23] Y. Okita and S. Yamawaki, "Conjugate heat transfer analysis of turbine rotor-stator system," ASME-paper GT-2002-30615, American Society of Mechanical Engineers, Orlando, Fla, USA, 2002.

[24] J. D. Heidmann, A. J. Kassab, E. A. Divo, F. Rodriguez, and E. Steinthorsson, "Conjugate heat transfer effects on a realistic film-cooled turbine vane," ASME-paper GT2003-38553, American Society of Mechanical Engineers, Orlando, Fla, USA, 2003.

[25] W. D. York and J. H. Leylek, "Three-dimensional conjugate heat transfer simulation of an internally-cooled gas turbine vane," ASME-paper GT2003-38551, American Society of Mechanical Engineers, Orlando, Fla, USA, 2003.

[26] T. Sugimoto, K. Nagai, M. Ryu, R. Tanaka, T. Kimura, and T. Nagatomo, "Development of a 20MW-class high-efficiency gas turbine L20A," ASME-paper GT-2002-30255, American Society of Mechanical Engineers, Orlando, Fla, USA, 2002.

[27] D. M. Kercher, "A film-cooling CFD bibliography: 1971–1996," *International Journal of Rotating Machinery*, vol. 4, no. 1, pp. 61–72, 1998.